

# Endoscopic Access Possibility in Maxillary Sinus Floor Augmentation - Part II

Desislava Stoyanova

Department of Periodontology and Dental Implantology, Medical University of Varna, Bulgaria

**Abstract:** *The aim of this study is to determine whether the largest share of visibility (SV) from the total viewing area of the maxillary sinus floor (MSF) is achieved when the endoscope enters in an anterior-posterior direction at 10 mm and an viewing angle of 45° at a comparable 30°, 45° and 70°. **Materials and methods:** An experimental study was conducted where SV of the maxillary sinus total surface area was measured on twenty 3D simulation models by using a built-in optics endoscope with angular visual axis deflected from 15° - 90°. **Results:** There was no statistically significant difference in SV of MSF total field of view relative to the medial, central, and distal endoscopic access openings at an endoscope penetration of 10 mm and an endoscope viewing angle of 45° and 70°,  $p \geq 0.05$ . SV of MSF total field of view was the same for all three openings and for both endoscope viewing angle of 45° and 70° and this SV was the highest compared with all other observations performed. **Conclusion:** This study offers valuable insights into the use of endoscopic techniques for minimally invasive maxillary sinus floor MSF augmentation. By analyzing the relationship between the endoscopes viewing angle, penetration depth, and field of view, the research confirms that optimal visibility is achieved at a 10 mm penetration depth with a 45° and 70° viewing angle.*

**Keywords:** endoscope, share of visibility, maxillary sinus floor, 3d models, endoscopically navigated surgery

## 1. Introduction

Medicine and dentistry development in recent years towards minimally invasive procedures has necessitated the increasing use of navigated endoscopic surgery (4).

There are not many reports in the literature focusing on dental implantology using endoscopically guided augmentation procedure to lift the MSF by using endoscopes with angled visual axis 0°, 30°, 45°, 70°, 90°, and 120° deviated from the instrument axis. The authors point to the endoscopically assisted MSF augmentation procedure as a minimally invasive technique with good visual control of the operative field, allowing detection of intraoperative Schneiderian membrane perforations during manipulation (1, 3, 5, 6, 7, 8).

Several years ago in our research for the first time, a visibility share of the total observation area of the sinus floor through an endoscope is examined, when entering it in the antero-

posterior direction in two positions 10 and 20 mm, observation angle 15°, 45° and 90°, as well as opening for the endoscopic approach through the fossa canina in three directions. In the research we found that the largest share of visibility from the total area of observation of the sinus floor is achieved when the endoscope enters in an antero-posterior direction at 10 mm and an angle of observation of 45° at comparable 15°, 45° and 90°. (2).

## 2. Materials and Methods

An experimental study was conducted on maxilla and maxillary sinuses three-dimensional simulation models. For the development of these three-dimensional simulation models, 20 preoperative CBCT images of patients who underwent sinus floor augmentation procedures with lateral approach were selected. The selected preoperative CBCT images for the development of the three-dimensional models were of 10 male and 10 female patients.

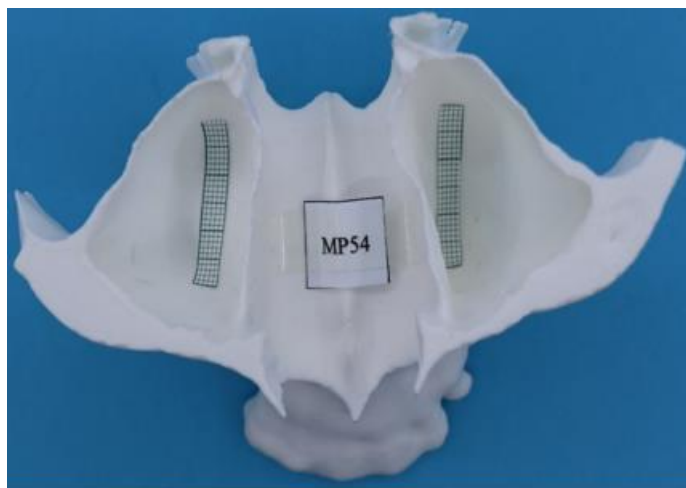


Figure 1

Using the CBCT image processing software "Planmeca Romexis", an image was generated to output an STL file. The prepared STL files of the three-dimensional models were printed using 3Dfactories' "Visions3Dprinter". The principle of operation of this printer is FDM (Fused Deposition Modeling) - the model is built by additively depositing a fused material (PLA - filament). The material is a filament with a diameter of 1.75 mm wound on a roll. The printer extruder has a diameter of 0.3 mm, the maximum printing speed is 80 mm/s. Ready STL files are prepared for printing by using "3Dfactories - Repetier - Host V1.0.6", and the same individual printing operating parameters are set for all 20 models to meet the needs of our task – model quality assurance - 0.08 mm (high quality), type of adhesion of the model to the table - Raft and maintenance of model by touching the table. The printing speed and the printing speed of the outer perimeter of the printed model is the same - 38

mm/s - slow type. The fill speed is 45 mm/s and the density is 60%. After completing the printing process, the 3D simulation models are subjected to cleaning of the support elements. The 3D simulation models are scaled 1:1 relative to the patients. In order to conduct the study of each 3D model in the antero-posterior direction, a millimetre paper was placed on each maxillary sinus floor, whose length was individualized according to the individual characteristics of each patient and its width is 5 mm (Figure 1).

On each maxillary sinus anterior wall, three openings, medial, central and distal, were performed by using a 5 mm diameter trocar with a distance of 8 mm between the centres of the holes. To locate the centre of the medial opening, the projection of the canine tooth 5 mm in vertical direction and then 5 mm in distal direction is taken as starting point (Figure 2).



Figure 2

On each sinus of the 3D models, a visibility fraction measurement of the maxillary sinus total surface area in the antero-posterior direction was conducted using a Karl Storz ENDOCAMELEON ENT HOPKINS Telescope with built-in optics with the angled visual axis deflected from 15° - 90° to the instrument axis.

Measurement of SV of the maxillary sinus total surface area was performed with the visual axis deflected to 30°, 45° and 70° to the instrument axis. SV of the maxillary sinus total surface area is established by relating the individual maxillary sinus length to the observed instantaneous length at the different visual axes of the selected 30°, 45° and 70° (Figure 3, 4 and 5).

To measure SV of the MSF total area, the endoscope was advanced in the antero-posterior direction 10 mm and 20 mm into each performed medial, central and distal opening of each sinus, which was observed at visual axes 30°, 45° and 70° to the instrument axis and the lowest focal angle.

The study data were re-downloaded, with a time interval between the two readings of nine months. All of the study data were used to investigate the accuracy of the measurements. The accuracy was tested with the intraclass correlation coefficient (ICC) using a 2-way random-effects model with absolute agreement. SV data of the maxillary sinus total surface area was analyzed against the endoscopic access opening, endoscope penetration depth, and endoscope viewing angle using IBM SPSS Statistics 25.

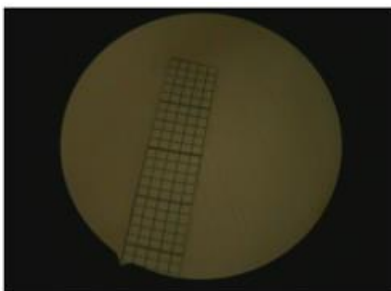


Figure 3

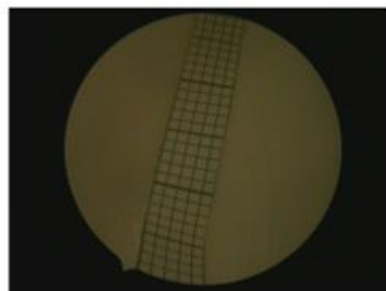


Figure 4

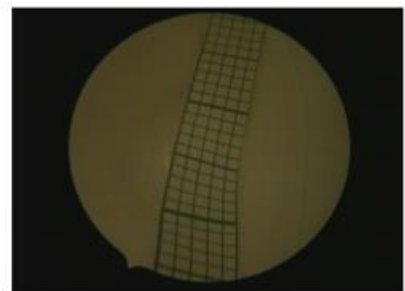


Figure 5

### 3. Results

Four observations were not included in the data analysis due to zero SV of MSF total observation area. This zero visibility was observed at the medial and distal openings with an endoscope penetration of 20 mm and a viewing angle with the endoscope of 30°. For medial are 1 and for distal - 3.

#### Data analysis to endoscopic access opening

The analysed data for SV of MSF total field of view to the endoscopic access opening are shown in table 1.

There was no statistically significant difference in SV of MSF total field of view relative to the medial, central, and distal endoscopic access openings at an endoscope penetration of 10 mm and an endoscope viewing angle of 45° and 70°,  $p \geq 0.05$ . SV of MSF total field of view was the same for all three openings and for both endoscope viewing angle of 45° and 70° and this SV was the highest compared with all other observations performed.

From the data analysis, there was a statistically significant difference in SV of the total field of view MSF from the medial, central and distal openings at an endoscope penetration of 10 mm and an viewing angle with the endoscope of 30° -  $p \leq 0.05$ , with SV of the total field of view of MSF decreasing from the medial ( $0.11 \pm 0.03$ ) to the distal opening ( $0.09 \pm 0.03$ ).

There was a statistically significant difference in the share of the total field of view of MSF to the medial, central, and distal openings at an endoscope penetration of 20 mm and an endoscope viewing angle of 30° -  $p \leq 0.05$ , with the share of the total field of view of MSF decreasing from the medial ( $0.05 \pm 0.02$ ) to the distal opening ( $0.04 \pm 0.02$ ).

There was a statistically significant difference in the share of the total field of view of MSF to the medial, central, and distal openings at an endoscope penetration of 20 mm and an endoscope viewing angle of 45°,  $p \leq 0.05$ , with the share of the total field of view of MSF decreasing from the medial ( $0.08 \pm 0.02$ ) to the distal opening ( $0.07 \pm 0.02$ ).

There was a statistically significant difference in the share of the total field of view of MSF to the medial, central and distal openings at an endoscope penetration of 20 mm and an endoscope viewing angle of 70° -  $p \leq 0.05$ , with the share of the total field of view of MSF increasing from the medial ( $0.09 \pm 0.02$ ) to the distal opening ( $0.08 \pm 0.02$ ).

#### Data analysis to endoscope penetration depth

The analysed data for SV of total field of view of MSF to the depth of endoscope penetration are shown in table 2.

There was a statistically significant difference of SV of the total field of view of MSF in the medial opening at an endoscope viewing angle of 30° to endoscope penetration depth of 10 and 20 mm, respectively,  $p \leq 0.05$ , with SV of the total field of view of MSF decreasing from 10 ( $0.11 \pm 0.03$ ) to 20 mm ( $0.05 \pm 0.02$ ) endoscope penetration depth.

There was a statistically significant difference in the share of the total field of view of MSF in the central opening at an

endoscope viewing angle of 30° to endoscope penetration depth of 10 and 20 mm, respectively,  $p \leq 0.05$ , with SV of the total field of view of MSF decreasing from 10 ( $0.10 \pm 0.02$ ) to 20 mm ( $0.04 \pm 0.02$ ) endoscope penetration depth.

There was a statistically significant difference in the share of the total field of view of MSF in the distal opening at an endoscope viewing angle of 30° to endoscope penetration depth of 10 and 20 mm, respectively,  $p \leq 0.05$ , with SV of the total field of view of MSF decreasing from 10 ( $0.09 \pm 0.03$ ) to 20 mm ( $0.04 \pm 0.02$ ) endoscope penetration depth.

There was a statistically significant difference in the share of the total field of view of MSF in the medial opening at an endoscope viewing angle of 45° to endoscope penetration depth of 10 and 20 mm, respectively,  $p \leq 0.05$ , with SV of the total field of view of MSF decreasing from 10 ( $0.12 \pm 0.02$ ) to 20 mm ( $0.08 \pm 0.02$ ) endoscope penetration depth.

There was a statistically significant difference in the share of the total field of view of MSF in the central opening at an endoscope viewing angle of 45° to endoscope penetration depth of 10 and 20 mm, respectively,  $p \leq 0.05$ , with SV of the total field of view of MSF decreasing from 10 ( $0.12 \pm 0.02$ ) to 20 mm ( $0.07 \pm 0.02$ ) endoscope penetration depth.

There was a statistically significant difference in the share of the total field of view of MSF in the distal opening at an endoscope viewing angle of 45° to endoscope penetration depth of 10 and 20 mm, respectively,  $p \leq 0.05$ , with SV of the total field of view of MSF decreasing from 10 ( $0.12 \pm 0.02$ ) to 20 mm ( $0.07 \pm 0.02$ ) endoscope penetration depth.

SV of the total field of view of MSF to the 10 mm depth of penetration was constant for all three endoscopic access holes at a 45° endoscope viewing angle, whereas the share of the total field of view of MSF to the 20 mm depth of penetration decreased from medial ( $0.08 \pm 0.02$ ) to distal ( $0.07 \pm 0.02$ ).

There was a statistically significant difference in the share of the total field of view of MSF in the medial opening at an endoscope viewing angle of 70° to endoscope penetration depth of 10 and 20 mm, respectively,  $p \leq 0.05$ , with SV of the total field of view of MSF decreasing from 10 ( $0.12 \pm 0.02$ ) to 20 mm ( $0.09 \pm 0.02$ ) endoscope penetration depth.

There was a statistically significant difference in the share of the total field of view of MSF in the central opening at an endoscope viewing angle of 70° to endoscope penetration depth of 10 and 20 mm, respectively,  $p \leq 0.05$ , with SV of the total field of view of MSF decreasing from 10 ( $0.12 \pm 0.02$ ) to 20 mm ( $0.08 \pm 0.01$ ) endoscope penetration depth.

There was a statistically significant difference in the share of the total field of view of MSF in the distal opening at an endoscope viewing angle of 70° to endoscope penetration depth of 10 and 20 mm, respectively,  $p \leq 0.05$ , with SV of the total field of view of MSF decreasing from 10 ( $0.12 \pm 0.02$ ) to 20 mm ( $0.08 \pm 0.02$ ) endoscope penetration depth.

SV of the total field of view of MSF to the 10 mm depth of penetration was constant for all three endoscopic access holes at a 70° endoscope viewing angle, whereas the share of the

total field of view of MSF to the 20 mm depth of penetration decreased from medial ( $0.09 \pm 0.02$ ) to distal ( $0.08 \pm 0.02$ ).

#### **Analysis of the data to the viewing angle with the endoscope**

The analysed data for SV of the total field of view of the maxillary sinus to the viewing angle with the endoscope are shown in table 3.

There was a statistically significant difference in SV of the total field of view of MSF for medial opening and endoscope penetration depth of 10 mm to viewing angle of 30°, 45°, and 70°, respectively,  $p \leq 0.05$ , with the highest share of visibility observed at a viewing angle of 45° and 70° ( $0.12 \pm 0.02$ ) and the lowest share at 30° ( $0.11 \pm 0.03$ ).

There was a statistically significant difference in SV of the total field of view of MSF for medial opening and endoscope penetration depth of 20 mm to viewing angle of 30°, 45° and 70°, respectively -  $p \leq 0.05$ , with SV increasing from viewing angle of 30° ( $0.05 \pm 0.02$ ) to 70° ( $0.09 \pm 0.02$ ).

There was a statistically significant difference in SV of the total field of view of MSF for a central opening and 10 mm endoscope penetration depth to viewing angle of 30°, 45° and 70°, respectively,  $p \leq 0.05$ , with the highest share of visibility observed at an viewing angle of 45° and 70° ( $0.12 \pm 0.02$ ) and the lowest share at 30° ( $0.10 \pm 0.02$ ).

There was a statistically significant difference in SV of the total field of view of MSF for central opening and endoscope penetration depth of 20 mm to viewing angle of 30°, 45° and 70°, respectively  $p \leq 0.05$ , with SV increasing from viewing angle of 30° ( $0.04 \pm 0.02$ ) to 70° ( $0.08 \pm 0.01$ ).

There was a statistically significant difference in SV of the total field of view of MSF for distal opening and endoscope penetration depth of 10 mm to viewing angle of 30°, 45° and 70°, respectively  $p \leq 0.05$ , with the highest SV observed at viewing angle of 45° and 70° ( $0.12 \pm 0.02$ ) and the lowest share at 30° ( $0.09 \pm 0.03$ ).

There was a statistically significant difference of SV of the total field of view of MSF for distal opening and 20 mm endoscope penetration depth to viewing angle of 30°, 45° and 70°, respectively  $p \leq 0.05$ , with SV increasing from viewing angle of 30° ( $0.04 \pm 0.02$ ) to 70° ( $0.08 \pm 0.02$ ).

#### **4. Discussion**

Comparing the results of the present study with those obtained in our study from a few years ago (2) we can confirm that the largest share of visibility from the total area of observation of the sinus floor is achieved when the endoscope enters from the medial opening in an antero-posterior direction at 10 mm.

Several years ago we found that the largest SV from the total area of observation of the sinus floor is achieved when the endoscope enters in an antero-posterior direction at 10 mm and an angle of observation of 45° at comparable 15°, 45° and 90° (2). Now in this study we found that SV of MSF total field of view was the same for both endoscope viewing angle of

45° and 70° and this SV was the highest compared with all other observations performed.

#### **5. Conclusion**

This study offers valuable insights into the use of endoscopic techniques for minimally invasive maxillary sinus floor MSF augmentation. By analyzing the relationship between the endoscopes viewing angle, penetration depth, and field of view, the research confirms that optimal visibility is achieved at a 10 mm penetration depth with a 45° and 70° viewing angle.

These findings align with prior studies, further establishing that the most effective endoscopic entry occurs in an anteroposterior direction through the medial opening. The results demonstrate that maintaining higher visibility through the appropriate angle and depth improves surgical control, reducing the risk of complications like membrane perforations. The consistency in observations between different openings and angles highlights the precision and reliability of this approach.

This research underscores the importance of endoscopic guidance in enhancing accuracy and control during MSF augmentation, supporting its continued adoption in dental implantology and related procedures. These findings pave the way for further improvements in surgical techniques and better clinical outcomes.

#### **References**

- [1] Berardini, Marco & Falco, Antonello & Amoroso, Cinzia & archivio, Lanfranco. (2015). Studio retrospettivo dei risultati clinici e radiologici di 69 rialzi di seno mascellare consecutivi associati a chirurgia endoscopica funzionale del seno (FESS). 10.11607/jomi.3757).
- [2] Desislava Stoyanova, Stefan Peev, Nikolay Sapundzhiev, Anjela Bakhova Endoscopic Access Possibility in Maxillary Sinus Floor Augmentation ; International Journal of Science and Research (IJSR), Volume 11 Issue 5, May 2022, DOI: 10.21275/SR22518162334, ISSN: 2319-7064(Online)
- [3] Engelke W, Deckwer I. Endoscopically controlled sinus floor augmentation. A preliminary report. Clin Oral Implants Res. 1997 Dec;8(6):527-31.
- [4] Engelke W., Beltran V., Endoscopic Techniques in Minimally Invasive Oral Surgery, Endo Press, 2014
- [5] Gandhi Y. Endoscopically monitored maxillary sinus augmentation – The chairside approach (Rationale and protocol). J Oral Biol Craniofac Res. 2020 Jul-Sep;10(3):247-252. doi: 10.1016/j.jobcr.2020.05.002. Epub 2020 May 12.
- [6] Hu YK, Yang C, Qian WT. Endoscopic-Assisted Sinus Floor Augmentation Combined With Removal of an Antral Pseudocyst of the Ipsilateral Maxillary Sinus. J Craniofac Surg. 2017 Sep;28(6):15491551.
- [7] Nkenke E, Schlegel A, Schultze-Mosgau S, Neukam FW, Wiltfang J. The endoscopically controlled osteotome sinus floor elevation: a preliminary prospective study. Int J Oral Maxillofac Implants. 2002 Jul-Aug;17(4):557-66.
- [8] Wiltfang J, Schultze-Mosgau S, Merten HA, Kessler P, Ludwig A, Engelke W. Endoscopic and ultrasonographic



evaluation of the maxillary sinus after combined sinus floor augmentation and implant insertion. Oral Surg Oral Med Oral Pathol Oral Radiol Endod. 2000 Mar;89(3):288-91. **Application**

**Table 1**

Opening	Penetration depth	Viewing angle	n observed region	Mean	SD	Median	Q <sub>1</sub>	Q <sub>3</sub>	IQR	Range	Min	Max	F (ANOVA)	P
Medial	10 mm	30°	40	0,11	0,03	0,11	0,09	0,13	0,04	0,12	0,05	0,17	7,88	0,001
Central			40	0,10	0,02	0,10	0,09	0,12	0,03	0,10	0,05	0,15		
Distal			40	0,09	0,03	0,09	0,07	0,11	0,04	0,12	0,02	0,14		
Medial	20 mm	30°	39	0,05	0,02	0,05	0,04	0,07	0,03	0,09	0,01	0,10	6,540051	0,002053
Central			40	0,04	0,02	0,04	0,03	0,06	0,03	0,07	0,01	0,08		
Distal			37	0,04	0,02	0,04	0,03	0,05	0,02	0,06	0,01	0,07		
Medial	10 mm	45°	40	0,12	0,02	0,12	0,11	0,14	0,03	0,10	0,08	0,18	1,998703	0,140111
Central			40	0,12	0,02	0,12	0,10	0,13	0,03	0,11	0,07	0,18		
Distal			40	0,12	0,02	0,11	0,10	0,13	0,03	0,08	0,08	0,16		
Medial	20 mm	45°	40	0,08	0,02	0,09	0,07	0,10	0,03	0,09	0,03	0,12	6,810391	0,001593
Central			40	0,07	0,02	0,08	0,06	0,09	0,03	0,08	0,03	0,11		
Distal			40	0,07	0,02	0,07	0,05	0,09	0,04	0,09	0,02	0,11		
Medial	10 mm	70°	40	0,12	0,02	0,12	0,11	0,14	0,03	0,11	0,07	0,18	0,602569	0,549094
Central			40	0,12	0,02	0,12	0,10	0,14	0,04	0,08	0,09	0,17		
Distal			40	0,12	0,02	0,12	0,10	0,13	0,03	0,10	0,08	0,18		
Medial	20 mm	70°	40	0,09	0,02	0,09	0,08	0,10	0,02	0,07	0,05	0,12	6,89638	0,001475
Central			40	0,08	0,01	0,08	0,06	0,09	0,03	0,05	0,05	0,10		
Distal			40	0,08	0,02	0,08	0,07	0,09	0,02	0,07	0,04	0,11		

**Table 2**

Penetration depth	Opening	Viewing angle	n observed region	Mean	SD	Median	Q <sub>1</sub>	Q <sub>3</sub>	IQR	Range	Min	Max	t test	P
10 mm	Medial	30°	40	0,11	0,03	0,11	0,09	0,13	0,04	0,12	0,05	0,17	9,336031	< 0,001
20 mm			39	0,05	0,02	0,05	0,04	0,07	0,03	0,09	0,01	0,10		
10 mm	Central	30°	40	0,10	0,02	0,10	0,09	0,12	0,03	0,10	0,05	0,15	11834,00	< 0,001
20 mm			40	0,04	0,02	0,04	0,03	0,06	0,03	0,07	0,01	0,08		
10 mm	Distal	30°	40	0,09	0,03	0,09	0,07	0,11	0,04	0,12	0,02	0,14	9,290335	< 0,001
20 mm			37	0,04	0,02	0,04	0,03	0,05	0,02	0,06	0,01	0,07		
10 mm	Medial	45°	40	0,12	0,02	0,12	0,11	0,14	0,03	0,10	0,08	0,18	8,426000	< 0,001
20 mm			40	0,08	0,02	0,09	0,07	0,10	0,03	0,09	0,03	0,12		
10 mm	Central	45°	40	0,12	0,02	0,12	0,10	0,13	0,03	0,11	0,07	0,18	9149,000	< 0,001
20 mm			40	0,07	0,02	0,08	0,06	0,09	0,03	0,08	0,03	0,11		
10 mm	Distal	45°	40	0,12	0,02	0,11	0,10	0,13	0,03	0,08	0,08	0,16	9,523000	< 0,001
20 mm			40	0,07	0,02	0,07	0,05	0,09	0,04	0,09	0,02	0,11		
10 mm	Medial	70°	40	0,12	0,02	0,12	0,11	0,14	0,03	0,11	0,07	0,18	7,216000	< 0,001
20 mm			40	0,09	0,02	0,09	0,08	0,10	0,02	0,07	0,05	0,12		
10 mm	Central	70°	40	0,12	0,02	0,12	0,10	0,13	0,03	0,10	0,08	0,18	9,325000	< 0,001
20 mm			40	0,08	0,01	0,08	0,06	0,09	0,03	0,05	0,05	0,10		
10 mm	Distal	70°	40	0,12	0,02	0,12	0,10	0,14	0,04	0,08	0,09	0,17	9,508000	< 0,001
20 mm			40	0,08	0,02	0,08	0,07	0,09	0,02	0,07	0,04	0,11		

Table 3

Viewing angle	Opening	Penetration depth	n observed region	Mean	SD	Median	Q <sub>1</sub>	Q <sub>3</sub>	IQR	Range	Min	Max	F (ANOVA)	P
30°	Medial	10 mm	40	0,11	0,03	0,11	0,09	0,13	0,03	0,12	0,05	0,17	3,346603	0,039
45°			40	0,12	0,02	0,12	0,11	0,14	0,03	0,10	0,08	0,18		
70°			40	0,12	0,02	0,12	0,11	0,14	0,03	0,11	0,07	0,18		
30°	Medial	20 mm	39	0,05	0,02	0,05	0,04	0,07	0,03	0,09	0,01	0,10	33,766	< 0,001
45°			40	0,08	0,02	0,09	0,07	0,10	0,03	0,09	0,03	0,12		
70°			40	0,09	0,02	0,09	0,08	0,10	0,02	0,07	0,05	0,12		
30°	Central	10 mm	40	0,10	0,02	0,10	0,09	0,12	0,03	0,10	0,05	0,15	7,815	< 0,001
45°			40	0,12	0,02	0,12	0,10	0,13	0,03	0,11	0,07	0,18		
70°			40	0,12	0,02	0,12	0,10	0,13	0,03	0,10	0,08	0,18		
30°	Central	20 mm	40	0,04	0,02	0,04	0,03	0,06	0,03	0,07	0,01	0,08	47,825	< 0,001
45°			40	0,07	0,02	0,08	0,06	0,09	0,03	0,08	0,03	0,11		
70°			40	0,08	0,01	0,08	0,06	0,09	0,03	0,05	0,05	0,10		
30°	Distal	10 mm	40	0,09	0,03	0,09	0,07	0,11	0,04	0,12	0,02	0,14	22,586	< 0,001
45°			40	0,12	0,02	0,11	0,10	0,13	0,03	0,08	0,08	0,16		
70°			40	0,12	0,02	0,12	0,10	0,14	0,04	0,08	0,09	0,17		
30°	Distal	20 mm	37	0,04	0,02	0,04	0,03	0,05	0,02	0,06	0,01	0,07	39,258	< 0,001
45°			40	0,07	0,02	0,07	0,05	0,09	0,04	0,09	0,02	0,11		
70°			40	0,08	0,02	0,08	0,07	0,09	0,02	0,07	0,04	0,11		

## Author Profile



**Desislava Kirilova Stoyanova**, PhD, Assistant Professor at Department of Periodontology and Dental Implantology, Medical University of Varna, Bulgaria, [dr.dess.stoyanova@gmail.com](mailto:dr.dess.stoyanova@gmail.com)